Korean J. Chem. Eng., 35(10), 2052-2064 (2018)
DOI: 10.1007/s11814-018-0119-4

pISSN: 0256-1115
eISSN: 1975-7220

Preparation and characterization of a novel calcium-conducting polymer inclusion membrane: Part I

Reza Darvishi*,*,†, Javad karimi Sabet**, and Mohsen Nasr Esfahany***

*Department of Chemical Engineering, Isfahan University of Technology, Isfahan 84156-83111, Iran
**Material and Nuclear Fuel Research School (MNFRS), Nuclear Science and Technology Research Institute, Tehran 14399-51113, Iran
***Polymer Engineering Department, Faculty of Petroleum and Gas (Gachsaran), Yasouj University, Gachsaran 75813-56001, Iran

(*Received 22 March 2018 • accepted 18 July 2018*)

Abstract−The preparation and characterization of a novel type of castor oil-based polymer inclusion membrane (PIM) was investigated, focusing on its flux and selective recovery of Ca^{2+} over competitive ions such as K^+, Na^+, and Mg^{2+}. The PIM contains a cross-linked high-molecular-weight green polyol (GPO) as a polymer base, benzene-18-crown-6 as a carrier, and an ionic liquid called 1-Butyl-3-methylimidazolium chloride as a plasticizer. GPO was first synthesized by a reaction between an epoxidized castor oil and a cellulose acetate, thereafter, cross-linked by isophorene isocyanate. The base polymer and the prepared PIM were characterized by gel permeation chromatography (GPC), Fourier transform infrared spectroscopy (FTIR), scanning electron microscope (SEM), atomic force microscopy (AFM), thermogravimetric analysis (TGA), and X-ray diffraction (XRD). The FTIR results indicate that oxirane groups in the epoxidized castor oil molecules reacted with the primary hydroxyl groups of cellulose acetate chains. The contact angle measurement hints at the hydrophobic characteristics of the prepared membrane. Compared to the PVC-, CA-, and PVDF-based polymer inclusion membrane, the cured GPO-based PIM, showed higher selectivity and flux of calcium ions with the same composition. The greater stability and significantly higher surface roughness are further favorable features of the novel PIM.

Keywords: Polymer Inclusion Membrane (PIM), Ionic Liquid, Green Polyol, Separation of Calcium Ion

INTRODUCTION

To diminish organic solvent use in the process of extraction, a state-of-the-art liquid membrane technology, the so-called polymer inclusion membrane (PIM), has been developed [1-4]. PIMs are prepared by casting a solution containing a carrier, a plasticizer and a base polymer dissolved in a volatile organic solvent. After the solvent evaporates completely, a thin, flexible and stable film is formed. PIM is a type of self-supported liquid membranes capable of carrying out the extraction and stripping processes simultaneously; meantime high selectivity for ion transport and convenient operation is provided [5-7].

Polymer inclusion membranes are being studied extensively in different areas of separation, especially, in carrier-mediated transport for selective separation and the recovery of metal ions from aqueous solutions [7-9]. Polymer inclusion membrane techniques have been exerted to selectively separate precious metals such as Hg, Cu, Ni, Zn, Pb, Cd, Cr(VI), Pu, Am, etc. [5,10-12] as well as small organic pollutants from aqueous phase with various types of carriers [1,3,13,14]. Furthermore, the chemical stability of PIMs is far better than other types of liquid membranes keeping the proper permeability (10 to 40 μmol/m^{2}s) and good selectivity [15]. In such a membrane system, distinct organic liquid phase does not exist and just a plasticizer component is embedded between polymer chains. For this potential advantage, the possibility of using very special extractants, which should be used at a very low and cost-effective amount, and thus the effectiveness of membrane separation system could be enhanced [7,13,16]. The main problem with PIMs is the low mechanical strength challenging potential feasible applications. So far, the PIM investigations have been confined to the only three major polymers: PVC, CA and recently PVDF, as base polymers. However, there is a large number of polymers being able to meet the characteristics to provide a flexible thin film, to support mechanically the membranes, to enhance the membrane stability and at the same time to generate a minimal hindrance to the transport of species within the membranes [17,18]. Consequently, some attempts have been made to design and to fabricate PIMs for offsetting the issue of low mechanical strength through manipulating the membrane matrix composition [19]. Therefore, choosing tailored compositions for PIMs is one of the main factors for membrane performance to separate a targeted solute. A combination of suitable plasticizers and thermoplastic polymers results in enhanced chemical stability, mechanical stability, and surface roughness on membranes, which in turn are found to increase the flux of facilitated diffusion [9,14]. Cellulose acetate (CA) is a polar and crystalline polymer. Due to the infusibility and insolubility properties, CTA is of propitious stability and excellent flux, making it particularly useful for PIM applications [20]. The slight hydrophilicity

†To whom correspondence should be addressed.
E-mail: r.darvishi@yu.ac.ir

characteristic and susceptibility of CA towards acid hydrolysis might be inherent drawbacks of cellulosic materials-based PIMs [19]. To alleviate these drawbacks, it is required to alter the structure of cellulosic materials to make them less accessible to hydrolysis [10,19].

The chemical change in the structure of polymer can be conducted so that not only all the unique characteristics of the polymer are maintained, but also its mechanical strength increases [21]. Membrane properties could be further tuned by using an ionic liquid instead of conventional plasticizers [12,21-23]. Also, ionic liquids (ILs) have been proposed as efficient plasticizers for PIMs, making the membrane softer and further stable in long-term exposure to extraction [24,25]. Imidazolium- and pyridinium-based ionic liquids have been the most popular ILs for the dissolution of cellulosic materials [24,26]. The goal of the present study was to design a proper recovery technology for selectively extracting a desired metallic cation or isotope from a feed solution. Since there is no work reported on calcium ion/isotope separation by polymer inclusion membrane, a novel PIM should be designed that, in addition to the advantages mentioned, has a high degree of selectivity for Ca^{2+} even over much smaller competitive ions [27]. In this regard, a high molecular weight green polyol (GPO) was first produced by reactions between oxirane groups of epoxidized castor oil and primary hydroxyl groups in cellulose acetate. The novel polymer inclusion membrane (PIM) contains GPO as the polymer support, a small amount of isophorone isocyanate (IPDI) as a crosslinker agent, Benzo-18-crown-6 (B18C6) as the carrier and 1-Butyl-3-methylimidazolium chloride (BMIMCl) as the plasticizer. This PIM was developed for the selective transport of Ca^{2+} over competitive cations (K^+, Mg^{2+}, Na^+) from aqueous chloride medium. To study the membrane performance in terms of selectivity and transport flux, the recovery of the calcium ion in the aqueous phase was examined. Here, Benzo-18-crown-6 was utilized as an effective carrier for the transport of alkali metals. The novel base polymer characteristics--molecuar weight, crystallinity, degradation temperature, glass transition temperature and morphology of its membrane as well as transport properties like selectivity and stability--were determined. In comparison of other similar PIMs, the novel membrane is believed to demand a lower amount of organic liquid, thereby reducing the simple diffusion of hydrated ions at a greater extent, and vice versa increasing the facilitated diffusion of ions across the membrane. The present work is further intended to serve as advanced research on calcium isotope enrichment, which will be published in future articles.

EXPERIMENTAL SECTION

1. Material

Sodium chloride (NaCl), potassium chloride (KCl), calcium chloride ($CaCl_2$) and magnesium chloride ($MgCl_2$), cellulose acetate (CA, the degree of acetylation of 2.87 and a molecular weight of ~78,000 g/mole), ionic liquid named 1-butyl-3-methylimidazolium chloride (BMIMCl), isophorone diisocyanate, and Benzo18Crown6 were purchased from Sigma-Aldrich. Castor oil, (Iodine value ≈90, the viscosity of 950-1050 mPas at 20 °C) was provided by M/s SD Fine-Chem Limited, Mumbai, India. Hydrochloric acid and N, N-dimethylacetamide (DMAC), isopropanol, fluoroboric acid and tetrahydrofuran were provided by Merck Company. All chemicals were used as received.

2. High Molecular Weight Green Polyol Preparation

2-1. Epoxidation of Castor Oil

A detailed description of the catalytic epoxidation reaction of castor oil has been provided elsewhere [23]. In brief, a mixture of castor oil, ethyl acetate, hydrogen peroxide (50%) as an oxidizing agent and Γ-alumina as a catalyst was heated in a 500 ml three-necked round-bottom flask equipped with a reflux condenser under vigorous mechanical agitation. The mixture for the reaction was stirred at 80 °C for 6 hr under a nitrogen (N_2) ambient. The epoxidized castor oil was purified by filtration and a simple Dean-Stark apparatus.

2-2. Synthesis of Green Polyol (GPO)

The green polyol was prepared by ring-opening reactions between epoxidized castor oil and cellulose acetate. First, the solution of CA in N, N-Dimethylacetamide (DMAc) was mixed along with isopropanol, and fluoroboric acid in a flask with a magnetic

Table 1. Fabricated PIMs samples with the related amounts of fluxes

Membrane name	Ionic liquid (g)	B18C6 (g)	Base polymer	Flux (10^{-3} mmol·cm^{-2}·h^{-1})	
				Average value	Standard deviation
MP	0.0	0.0	1 gr CA	.25	0.01
GMN	0	0	1 gr GPO (non-crosslinked)	.05	0.00
GMC1	0	0	1 gr GPO (cross-linked)	0.00	0
GMC2	.5	0	1 gr GPO (cross-linked)	0.79	0.07
GMC3	1	0	1 gr GPO (cross-linked)	1.81	0.11
GMC4	1.5	0	1 gr GPO (cross-linked)	2.91	0.13
PIMC5	1.5	.25	1 gr GPO (cross-linked)	17.45	0.37
PIMC6	1.5	.5	1 gr GPO (cross-linked)	23	0.53
PIMC7	1.5	.75	1 gr GPO (cross-linked)	43.4	1.74
PIMC8	1.5	1	1 gr GPO (cross-linked)	6.08	0.24
CA-PIM (as reference)	1.5	.75	1 gr CA	21.81	0.9
PVDF-PIM	1.5	.75	1 gr PVDF	44.01	0.02
PVC-PIM	1.5	.75	1 gr PVC	41.3	0.04

stirrer at 60 °C. The epoxidized castor oil obtained in the previous stage was added dropwise to the mixture with vigorous stirring. The molar ratio of oxirane group in epoxidized castor oil to the primary hydroxyl group in cellulose acetate (which was determined by the method provided by [28]) was regulated to be 2. The reaction is nearly completed at about 2 hr. The viscous polyols were obtained after the removal of organic solvent using rotavapor and vacuum drying.

3. Membrane Preparation

The GPO-based cross-linkable membrane sample was prepared by solution casting as follows. The different proportion of GPO and BMIMCl ionic liquid and B18C6 was dissolved into the N, N-dimethylacetamide (DMAc, 10 mL) according to composition data given in Table 1. The corresponding mixture of each membrane was stirred for 24 hr at room temperature, then, crosslinking agents (isophorone diisocyanate and dibutyl tin dilaurate) were incorporated into the resulting solution. After further stirring for 20 min, flat sheet membranes were prepared using an aluminum casting knife containing a steel blade which was precisely regulated to create a narrow gap between the blade and the glass plate onto which the film was cast. After casting the polymer solution upon a smooth glass plate, they are left in a desiccator at the temperature of the ambient air allowing for solvent evaporation and for the deposition of a uniform thin film with a thickness circa 35-40 micrometer. Membranes, formed on a glass plate, could be effortlessly peeled off by soaking in a deionized (DI) water bath at room temperature. For transport experiments, the dry membrane was cut to the proper dimensions (circular membranes with 5 cm radius) to be configured into flat-sheet membrane modules.

4. Characterization

The molecular weight and its distribution were measured by gel permeation chromatography (ALC, Waters) with the use of 1 ml of 0.5% solutions of GPO and CA in tetrahydrofuran at 40 °C, and a 1 mL/min flow rate. Field-emission scanning electron microscopy (FESEM, XL30, Philips and atomic force microscopy (AFM, Park Scientific) were used to obtain information regarding the surface morphology of prepared membranes. To view membrane cross-section of the PIMs, the membrane samples were frozen in liquid nitrogen (70 K) and rapidly fractured. The samples were mounted on the aluminum stub using double-sided adhesive tape, thereafter coated with gold by sputtering. To estimate the surface tension and the wettability of membranes, contact angles were recorded with a goniometer (KRÜSS DSA 10-MK2) equipped with a special optical system coupled with a CCD camera. The contact angles of water were measured at least five various positions on the same sample surface; thus, the mean amount of the contact angle was reported. To investigate the type of functional groups in prepared samples, the Fourier transform infrared spectroscopy (FTIR) spectra were recorded using IR Affinity-1 (Shimadzu) spectrometer in the wavenumbers ranging from 400–4,000 cm^{-1} in transmission mode with an accumulation of 32-time scans and resolution of 2.0 cm^{-1}. The crystallinity of the membranes was evaluated using Philips, model X-pert X-ray diffractometer operating at 40 Kv, using Cu as the radiation source; the scans were obtained using a scan step size of 0.03 with a scan step time of 0.25 s. The thermogravimetric analyses were achieved using a SETARAM TG 96, thermal analysis instrument. A 3 mg sample of membranes was dried at 100 °C to remove moisture for 30 min under vacuum circumstance, afterward, programmed from 30 to 800 °C at the rate of 10 °C/min under the nitrogen ambient. As the conductivity of the water which membrane is in contact with, could be used as a measure of the leakage and/or losses of membrane phase components during transport process, the stability of the polymer inclusion membranes in some experiments, was checked by using a conductometer. Inside a beaker, 500 mg of the membrane samples was soaked in the deionized water at room temperature for 24 h and left under magnetic stirring at 450 rpm. The conductivity of the water was recorded after 24 hours at 25 °C as an amount of the crown ether and released ionic liquid content. The water content percentages were measured by soaking a 5 g-sample in 50 mL-distilled water for 48 h, at room Temperature. The sample was brought out, drained and excess water was removed using a tissue paper. The weight of the swollen sample was measured. The water content was determined by below equation:

$$\text{Water content (\%)} = \frac{\text{Weight after soaking} - \text{Weight before soaking}}{\text{Weight before soaking}}$$

Stress-strain data of the membranes were obtained by means of Zwick 1445 Universal Testing System, with a head force of 500 N. At low stress levels extension rate was 1 mm/min. The rate of extension was then set to 50 mm/min until the breaking of the samples. The membrane samples were cut into dumbbell shapes with length of 82 mm and width of 10 mm. The measurements were carried out at room temperature.

5. Transport Analysis

To determine an optimal composition of PIM to selectively recover Ca^{+2} as well as explore the mechanism of extraction, membranes with varying material compositions were examined for the separation of an equimolar Na^{+}, Ca^{2+}, Mg^{2+}, K^{+} solution in the feed phase. Polymer inclusion membrane transport experiments were carried out in a two-compartment glass cell for the feed and stripping phases with 200 cm^3 volume each. A 5 cm diameter PIM was sandwiched between the circular openings of the two compartments. The same molar concentration of the alkali metal salt (0.01 M) was fed to the source chamber and the pH was adjusted to be basic by tris(hydroxymethyl) aminomethane (0.05 M). The stripping aqueous phase consisted of distilled deionized water. Each compartment was continuously homogenized using a stirring magnetic bar at a stirring speed of 600 rpm. Fig. 1 presents schematically the flat sheet module used here.

Samples of 2 ml were taken from both aqueous phases after every eight hours and analyzed for cation concentration using a PerkinElmer Elan 9000 ICP/MS System. Each experiment was repeated at least three times and the average value was reported as the final upshots.

6. Flux and Selectivity Calculations

Cation flux (J_i, μmol m^{-2} s^{-1}) through the membrane could be calculated using an equation as below [29]:

$$J_i = \frac{V}{A}\frac{dC_i}{dt} \quad (1)$$

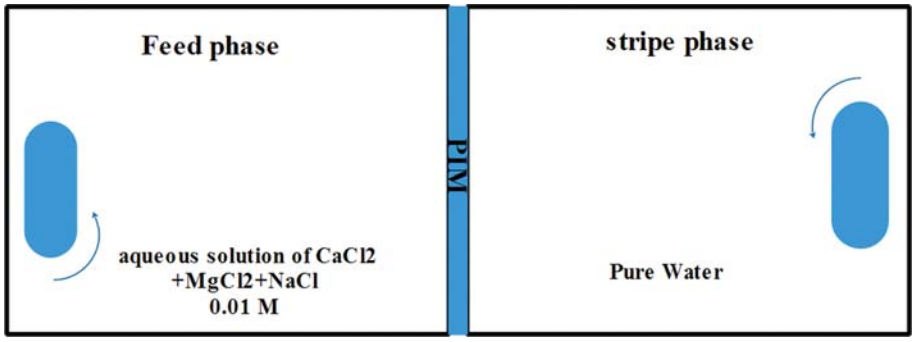

Fig. 1. Schematic of the flat-sheet membrane module used for transport experiments.

In which A is the effective membrane area (cm^2) and V is the aqueous phase volume (mL). dC/dt is the metal ions concentrations change with time. The selectivity could be defined as the relative tendency of two different ions to cross the membrane [15]:

$$\alpha_{i,j}=\frac{J_i\Delta C_j}{J_j\Delta C_i} \quad (2)$$

where ΔC is the concentration difference of each cation between two compartments after certain times. The flux results of different membranes are given in Table 1.

RESULTS AND DISCUSSION

1. Membrane Characterization

The epoxidation reaction of castor oil was characterized by FTIR absorption spectrum shown in Fig. 2.

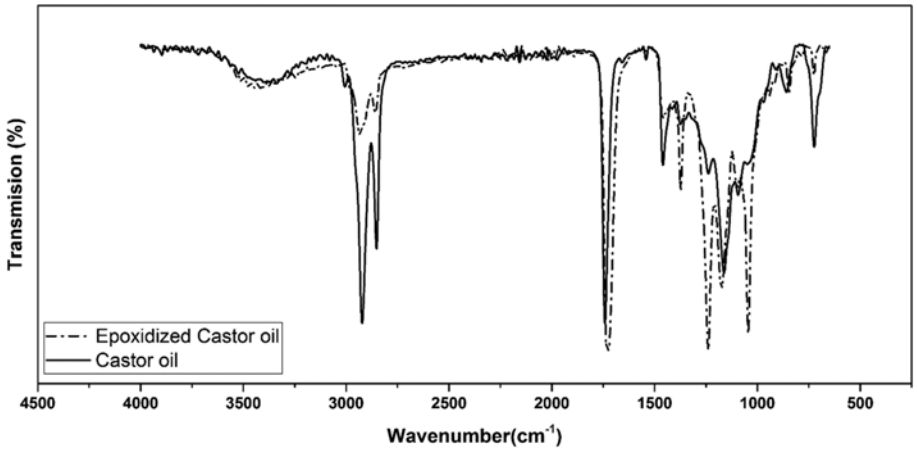

Fig. 2. FTIR spectrum related to castor oil and epoxidized castor oil.

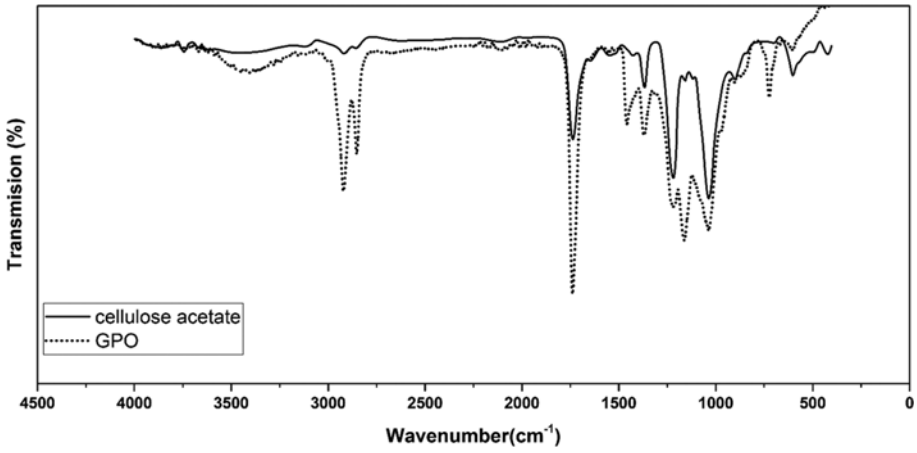

Fig. 3. A comparison between FTIR spectra corresponding to GPO and CA.

As observed, the C=C absorption band at 3,009 cm is fully disappeared and a new peak at 846 cm^{-1} related to the epoxy group absorption appeared. The sharp intense peaks at 1,045 and 1,246 cm^{-1} were assigned to the symmetrical axial bending and stretching of the oxirane ring, respectively.

Fig. 3 exhibits the ATR-FTIR spectra of the polyol prepared from the oxirane ring-opening of epoxidized castor oil with CA.

The bands of 2,986 cm^{-1} and 2,936 cm^{-1} were assigned to the stretching vibration of C-H in CH_2 and CH_3. The adsorption at 1,750 cm^{-1} was assigned to the stretching vibration of C=O in CA. As could be observed in the figure, oxirane absorption at 823 cm^{-1} nearly disappears. The appearance of the peak at 3,392 cm^{-1} reveals that the epoxy groups in epoxidized castor oil are ring-opened by CA and replaced by hydroxyl groups. Comparing two ATR FTIR spectra of CA and GPO membranes, ranging from 1000 to 1250, it could be found that the relative intensities of ether bond stretching increases in GPO. This could be explained by considering the conversion of hydroxyl groups in macromolecular chains of cellulose acetate to ether groups. Fig. 4 represents the recorded FTIR spectra related to the cured GPO-based samples.

The absence of the band in the range of 2,260 to 2,310 cm^{-1} confirms the absence of free NCO group in membrane structure, indicating that the reaction of the isophorone diisocyanate with hydroxyl groups was completed. The presence of vibrational bands at 1,072 cm^{-1} (C-N stretching vibrations), 1,123 cm (C-O stretching vibrations), 1,557-1,580 cm^{-1} (C-N stretching and N-H bending), 1,600 cm^{-1} (C-C stretching vibration), 1,720-1,730 cm^{-1} (C-O stretching vibrations from urethane groups), 2,857-2,925 cm^{-1} (CH_2 symmetric and anti-symmetric stretching vibrations) and 3,378 cm^{-1} (free O-H and N-H stretching from urethane group stretching vibrations) show the formation of urethane linkage, NH-COO in the isophorene diisocyanate cured GPO-based samples. IR absorption frequencies assignments to the carrier (B18C6), the ionic liquid (BMIMCl) and the corresponding PIM cured-(GPO/BMIMCl/B18C6) are represented in Fig. 5.

Comparing the peaks attained from the FTIR spectra of PIM and individual constituents of the membranes, it could be concluded that no chemical interaction occurred during the membrane preparation process and all the membrane constituents persisted as pure components within the membrane.

Now it was evident that the reaction between CA and epoxidized castor oil had taken place, it was time to determine the molecular characteristics of the new product (GPO). Fig. 6 shows the comparison of the molecular weight distribution of GPO and CA

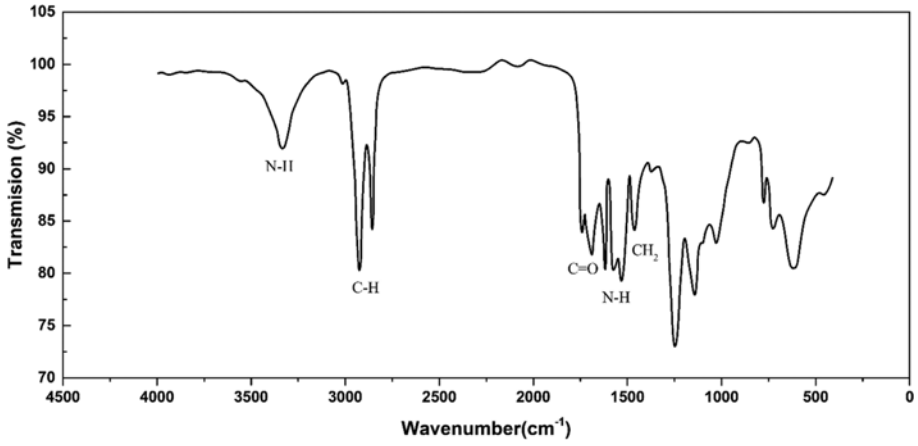

Fig. 4. FTIR spectrum assigned to GPO.

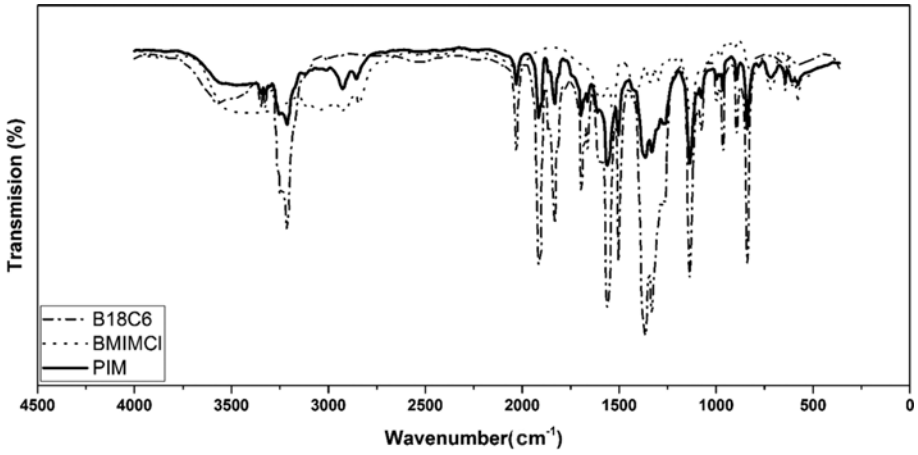

Fig. 5. Comparing the FTIR spectra of GPO-based PIM (PIM7) and the constituting components.

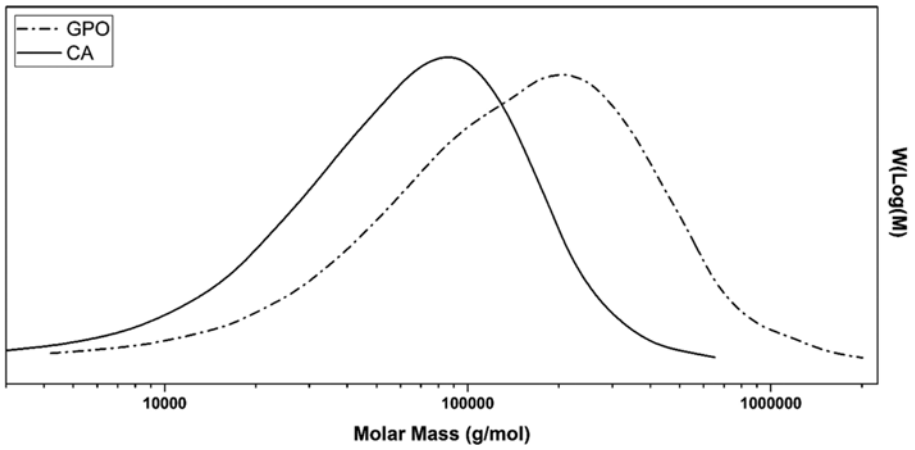

Fig. 6. Gel permeation chromatography results of GPO and CA chains.

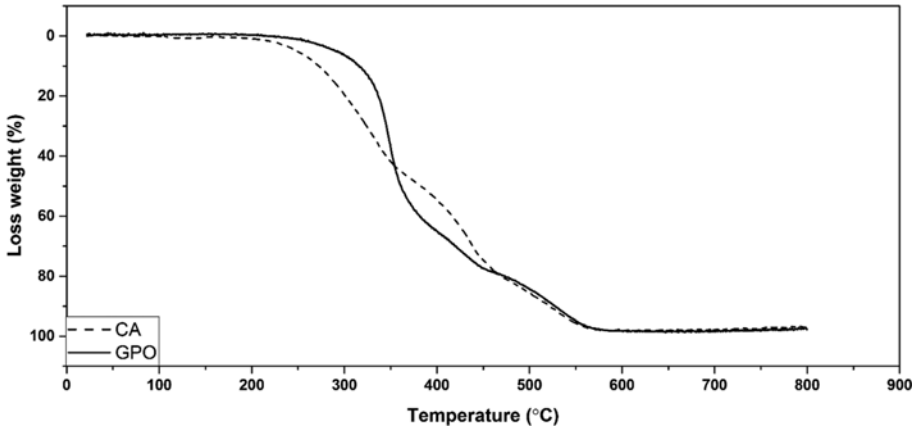

Fig. 7. Collating the TGA analyses of GPO-based (GMC) and CA-based (MP) membranes.

samples. As can be seen, there is a significant change in the MW and its distribution (polydispersity index) when CA is reacted with epoxidized castor oil. The presence of multiple reactive epoxide sites in epoxidized castor oil allows for reaction with several CA chains, resulting in extending the chain length and thereby increasing MW and MWD.

The traces of losing weight and differential thermogravimetry (DTG) of the synthesized polymer GPO are compared with cellulose acetate in Fig. 7. As shown, the data includes onset temperature where slow degradation with higher activation energy occurs, and the most rapid decomposition temperature where complete degradation with lower activation energy happens.

The early decomposition peak, which is attributed to the thermal cleavage of ether and ester groups present in both polymer

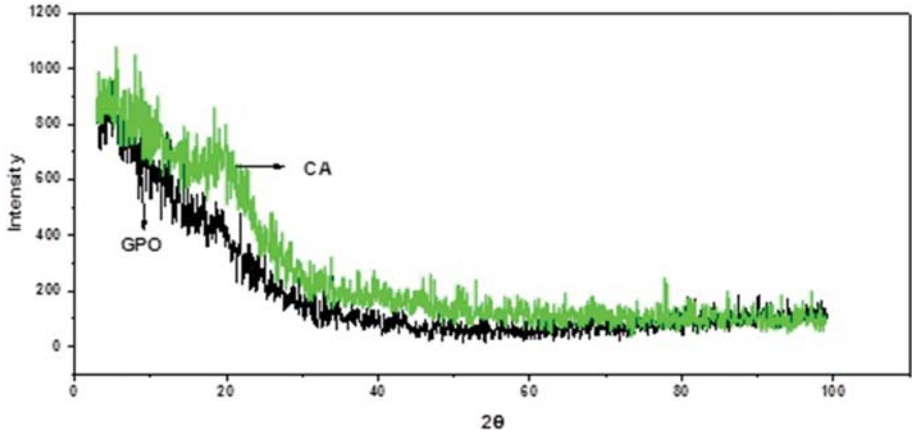

Fig. 8. XRD spectra related to CA-based (MP) and GPO-based (GMC) membranes.

matrices, occurs faster for cellulose acetate. Green polyol samples also exhibit a wider late decomposition peak shifted toward higher values of temperature. This implies that the thermal stability of cellulose acetate could be improved by the formation of the semi-cross-linked structure of CA with epoxidized castor oil.

Fig. 8 illustrates a comparison between XRD patterns of cellulose acetate and GPO samples. The patterns made bare changes in the crystal strata distances with the reaction of cellulose acetate and epoxidized castor oils. While CA sample registered a (001) diffraction peak at about $2\theta=20^{o}$, the GPO sample demonstrates no XRD peak, indicating the fully amorphous structure in GPO. The reaction between castor oil and cellulose acetate removes the interchain order required for the formation of crystalline regions, likewise, increases the gap between the chains; the castor oil is able to internally plasticize cellulose acetate matrix. This amorphous structure of polymer matrix could positively affect the flux of the desired solute in the subsequent transport process.

Fig. 9 shows the SEM pictures of the surface morphology of both pure CA and GPO films and their corresponding membrane with the same composition of the ionic liquid. While a smooth surface was observed in the case of the pure CA and CA/IL membrane, the GPO-based membrane in the presence of plasticizer of BIMIMCl shows a significant change in surface topography compared with pure GPO film. The GPO film presented a significant increase in roughness after introducing the ionic liquid into the polymer matrix.

These rough regions may have occurred due to different natures of the neighboring spotted areas filled by the carrier, plasticizer and polymer matrix on the membrane surface. The higher the roughness, the greater the difference in chemical nature of two neighboring spot areas is. The surface roughness of GPO-based PIM could enlarge the effective contact surface area, leading to higher efficiency of the ion transport process.

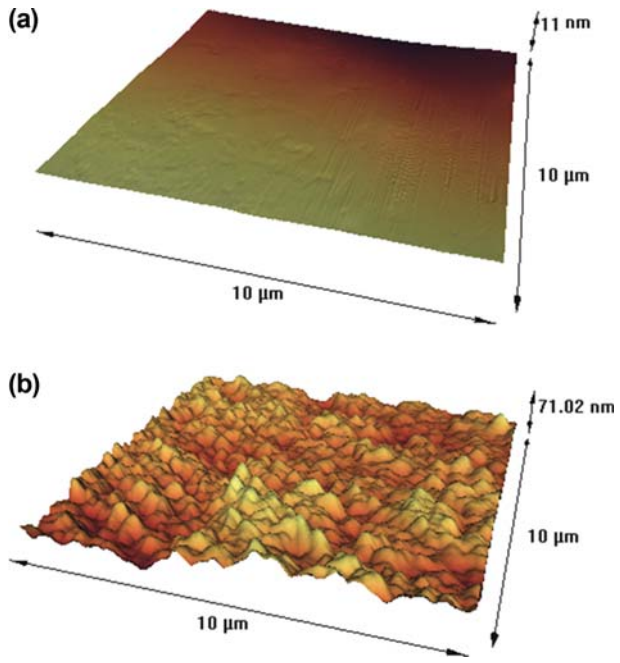

Fig. 10. AFM images of (a) CA-based (MP) and (b) GPO-based (GMC) membranes.

AFM images of the membrane prepared by both CA (MP) and GPO (GMC) in the three-dimensional format of 10 μm×10 μm

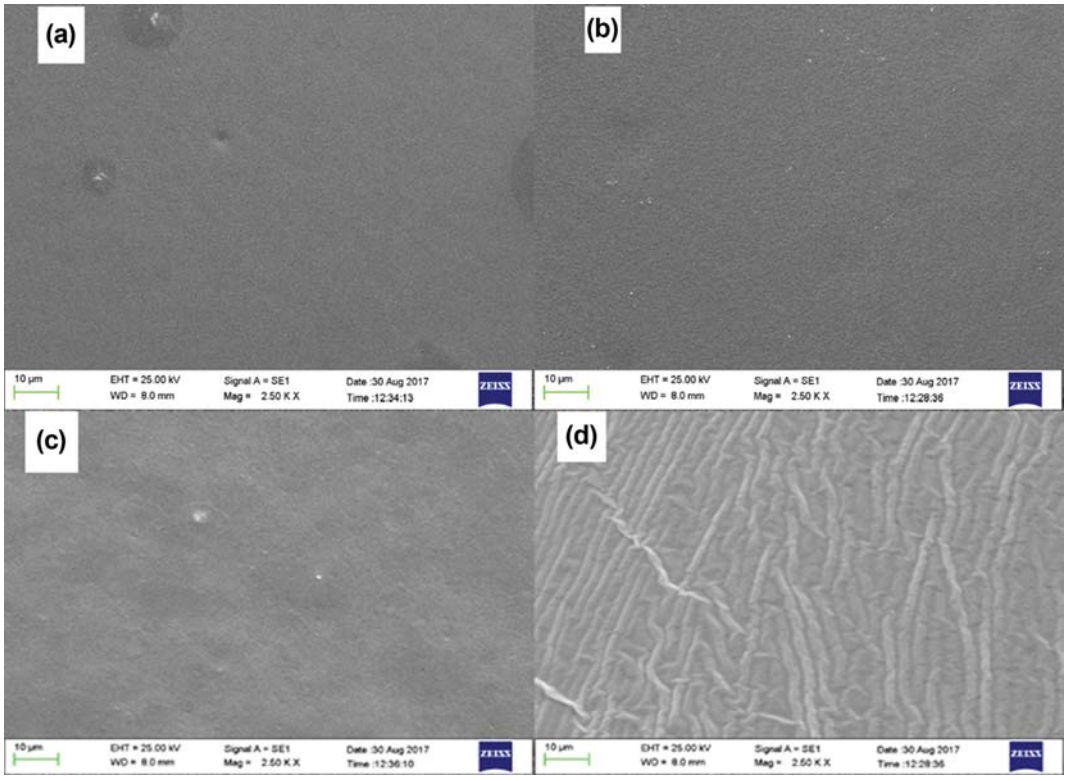

Fig. 9. SEM images related to membranes based on (a) CA (MP), (b) GPO (GMC), (c) CA/IL (CA-PIM) and (d) GPO/IL (PIM7).

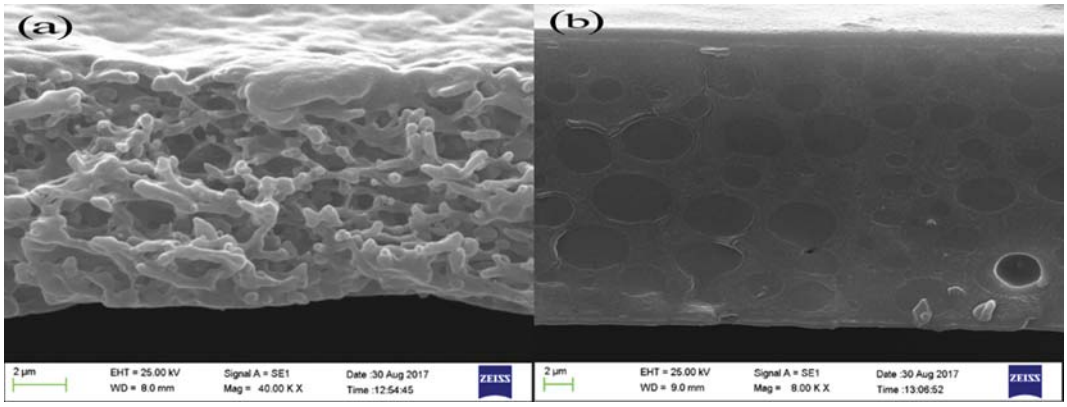

Fig. 11. SEM images of PIMs cross sections based on (a) CA (CA-PIM) and (b) GPO (PIM7).

are shown in Fig. 10. Mean roughness values for the samples are obtained as 1.6 and 11.2, respectively.

As deducible from Fig. 10, CA film has a very smooth surface, whereas the GPO based membrane exhibits large-scale surface roughness. Also, the roughness of these membranes after adding ionic liquid and crown ether (i.e., CA-PIM and PIM7) is examined and obtained as 6.1 and 23.4, respectively. It was found that the migration of plasticizer molecules to the membrane surface and the crystallization of the carrier molecules can increase roughness [20].

Fig. 11 indicates the cross-sectional SEM images of the membranes, CA-PIM, PIM7. Both cellulose acetate and cured GPO-based membranes generate a porous membrane in the presence of ionic liquid in membrane bulk and a dense layer in membrane surface.

While an open internal porous structure is observed in the case of CA/IL, GPO/IL formed a distinguished closed-cell membrane. As shown in Fig. 11, the pore size and porous structure of CA/IL membrane are changed by changing the chemistry of CA chain with epoxidized castor oil. Closed porous networks consisting of the ionic liquid help membrane maintain chemical stability; thus, no organic liquid leaks into aqueous feed and strip phases. The determined pores correspond well with the above results of the roughness values in the membranes.

Fig. 12 shows contact angle measurement applied to investigate the hydrophilicity of the material surfaces. Even though the contact angle of the GPO film is 79±1, the contact angles of PIMs increased to 105. This phenomenon could be the result of changes in surface morphology and the hydrophobic of ionic liquid in membranes. In the hydrophobic region, the contact angle was observed to increase if the surface roughness increased. Contact angles at rough hydrophobic surfaces are higher because the drop edge is arrested by the border of the grooves and the liquid does not penetrate the scratches.

Fig. 13 compares the water content percentage of the cured GPO film with CA membrane. It is clear that the GPO membrane had significantly lower value of water content percentage than the CA film. The lower water content percentage of the GPO membrane than that in case of CA may be due to cross-links between the polymer chains, which decreased the diffusion of water through the polymer matrix. Moreover, the chemical bond of hydrophobic castor oil molecules with CA chains increases its hydrophobicity. All of this confirms that hydrated cations may not passively diffuse across the GPO membrane via simple diffusion.

Fig. 14 illustrates the stress-strain curves for the CA- and GPO-

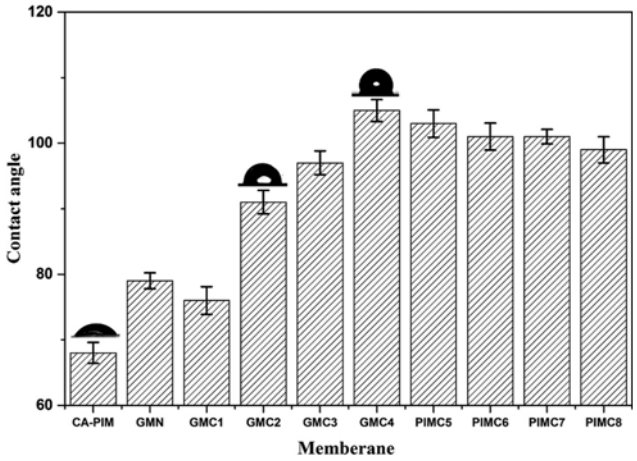

Fig. 12. The values of contact angles corresponding to various fabricated membranes.

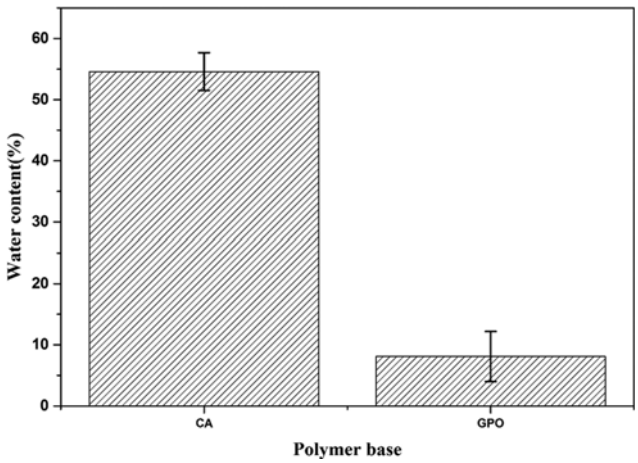

Fig. 13. Comparison of water resistance of GPO (GMC) and CA (MP).

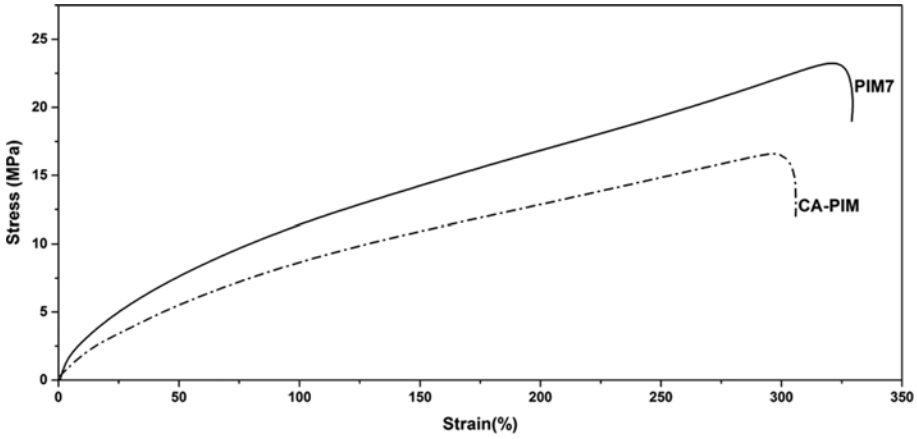

Fig. 14. Stress-strain curves for two CA- and GPO-based membranes. The composition of the membranes are the same.

based membranes. The moduli of elasticity were determined to be 59 and 96 MPa, respectively, for CA-PIM and PIM7.

As can be seen, the GPO-based PIM, due to intermolecular crosslinking, exhibit higher modulus, greater ultimate strength, and higher elongation at break and in general, better mechanical properties.

2. Effect of Curing GPO on Cation Transport

To examine the influence of the cross-linking on the flux of Ca^{2+}, a non-cross-linked GPO-based PIM was compared with cross-linked one in the absence of any other membrane components, i.e., carrier and plasticizer. In general, cross-linking between polymer chains could affect the chain mobility and spaces between molecules, thereby affecting transport properties [30]. The latter means that ion transport across the membrane could be performed when lattice voids are larger than hydrated ions radii. Cellulose acetate is a hydrophilic polymer with two types of regions: crystalline and amorphous [24,30-32]. Hydrated cation ions could be absorbed via hydrogen bonding in the amorphous region where void spaces between polymer chains are sufficient to allow the ions to transport. Table 2 shows that CA itself is not completely impermeable to Ca^{2+} whereas GMN and especially GMCs are. Chemical modification of cellulose acetate by castor oil and especially cross-linking with isophorone diisocyanate increases membrane hydrophobicity lowering the affinity of Ca^{2+} towards the membranes (GM serious). In other words, Ca^{2+} cannot pass through cross-linked GPO-based PIM by simple diffusion, and if ion transport is going to occur, it has to be in form of carrier-mediated transport. This unique feature of the membrane could contribute to the higher selectivity of the membrane. The advantages of cross-linked membrane become more obvious when its chemical stability is compared with other forms of liquid membranes. While CA- and non-cross-linked GPO-based PIM show a conductivity of 15 and 36 μs/cm, respectively, under aforementioned test conditions, the cured samples do not reveal any ionic liquid or crown ether leakage. This indicates that the cross-linking of polymer matrix can help organize membrane components into localized areas.

Table 2. Selectivity amounts of PIMs

Membrane	$\alpha_{Ca/K}$	$\alpha_{Ca/Na}$	$\alpha_{Ca/Mg}$
PIMC5	17	47.4	162.7
PIMC6	68	189.8	651.7
PIMC7	88.8	247.5	856.1
PIMC8	22.5	62.3	213.4
PIMP	16.7	32.6	78.67

3. Effect of Ionic Liquid Incorporation on Cation Transport

When imidazolium ionic liquid is introduced into membrane as the plasticizer, PIM becomes more flexible and the ion flux increases. This could be because interaction forces between polymer chains in the membrane structure are reduced by adding ionic liquid; consequently, void spaces between polymer molecules are increased. Table 2 presents the influence of the content of ionic liquid on the flux of Ca^{2+} across the PIMC in the absence of carrier. As can be shown, the flux of Ca^{2+} across the membrane increases steadily with increasing the content of the ionic liquid. Therefore, a ratio of ionic liquid to polymer base of 1.5 is considered to be optimum for final PIM with the presence of carrier (GMC1-4).

4. Effect of Crown Ether Incorporation on Cation Transport

The influence of B18C6 on the ion flux and selectivity was examined by preparation of membranes with an ionic liquid to modified cellulose acetate ratio of 1.5 with different B18C6 content. An equimolar mixture of Ca^{2+}, Mg^{2+}, Na^{+}, and K^{+} was used in the feed phase. As shown in Table 2, the flux for Ca^{2+} of PIMs containing B18C6 increased by 20-fold compared to PIMC-3 containing only modified CA and an ionic liquid. Flux in the presence of carriers is dependent on the size of ions which should exactly fit into the cavity of crown ether to form a complex. If an ion has the same size as the cavity of 18-crown-6, it has more probability to bind to the crown ether and thus to transport. For any content of B18C6, the flux of Ca^{2+} was greater than for other cations. As can be seen from Fig. 15, PIMC7 with a content of B18C6 of 0.75 gr, presented a maximum flux of cations across the membrane.

The downward trend of the fluxes above this content of B18C6 can be explained by the fact that B18C6 compound was not soluble in membrane media and tended to form crystals in higher concentration than 0.75 gr/1 gr. Moreover, to perceive the impact of the base polymer upon the amount of ion transport, a CA-based

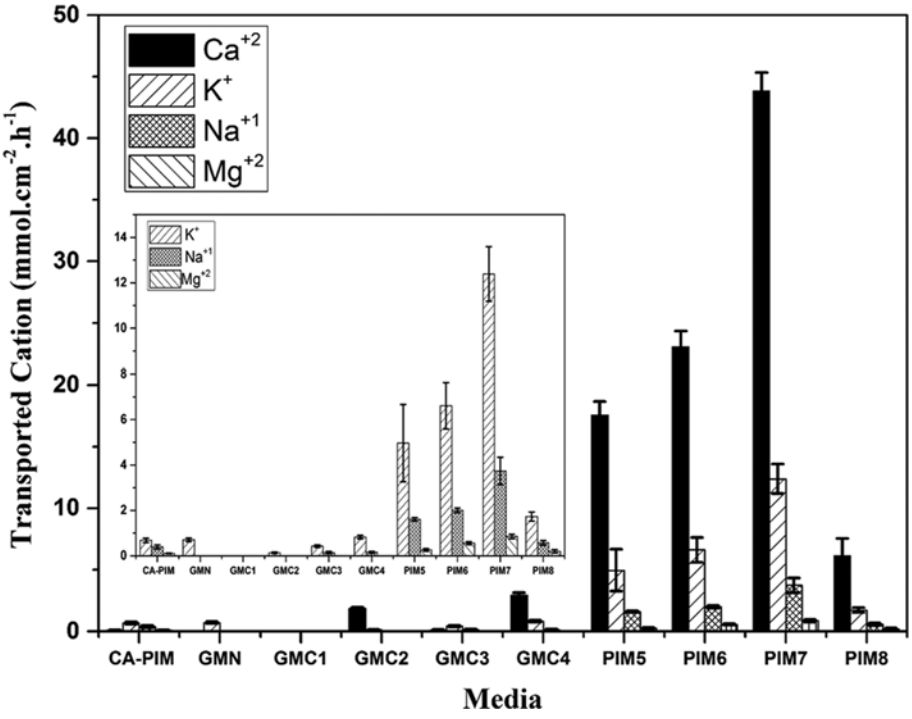

Fig. 15. Bar graph associated with the flux amount of each fabricated membrane.

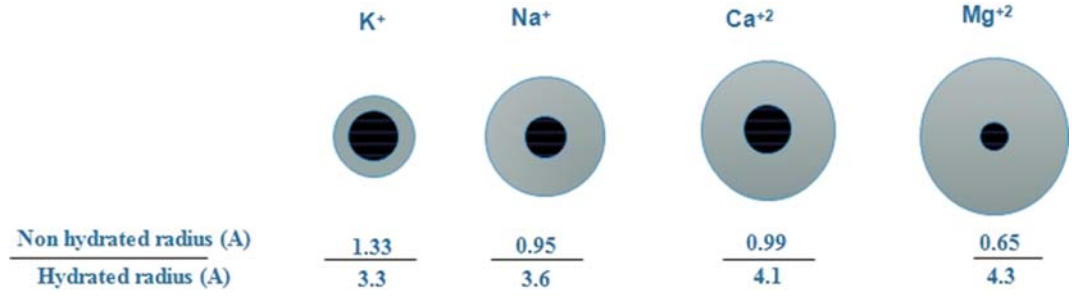

Fig. 16. Comparison of the non-hydrated and hydrated radius of cations [8].

PIM was fabricated as a reference with a composition like PIMC7. As is evident, the flux of a PIM with the optimum composition based on GPO is circa twofold a CA-based PIM. At this juncture, this phenomenon could be justified through the plasticizing aspect of the castor oil reacting with CA within GPO. Furthermore, to perceive the impact of base polymer on the flux value of transport, a CA-based PIM as a reference was fabricated with a composition like PIMC7. As is evident, the flux of a GPO-based PIM with the optimum composition is circa twofold a CA-based PIM. At this juncture, this phenomenon could be justified through the plasticizing aspect of the castor oil reacting with CA within the GPO.

5. Selectivity

Selectivity was calculated comparing the content of Ca^{2+} transported in comparison with the content of competitive cations transported after the course of the experiment.

As shown in Table 1, the optimum content of B18C6 to achieve the highest selectivity of Ca^{2+} over other competitive cations corresponds to the content required for the greatest flux of cations. This observation suggests that the main mechanism for the ion transport is the carrier-mediated diffusion, and the PIMs show almost a similar behavior against the simple diffusion of cations. So, in this membrane composition, metal-ligand electrostatic effect outweighs solvation effects. The ease of simple diffusion of the cations strongly depends on the ion size (Fig. 16) and the hydrophobicity of the membrane.

Cations with larger non-hydrated radii or smaller hydrated radii have greater simple diffusion power to pass across a membrane (Mg^{2+} and Ca^{2+} have larger hydrated ion radii compared to alkaline metal ions (Na^{+}, K^{+})). This shows that the most important competitive cation for Ca^{2+} is K^{+} which is due to its small size of hydration shell giving small effective diameter in aqueous solution (3.3 Å). The selectivities of two samples of PIMC7 and CA-PIM were also compared to indicate the role of hydrophobicity in the membrane. GPO-base PIM is further selective compared with pure CA-based PIM due to the more hydrophobic structure of GPO-based PIM.

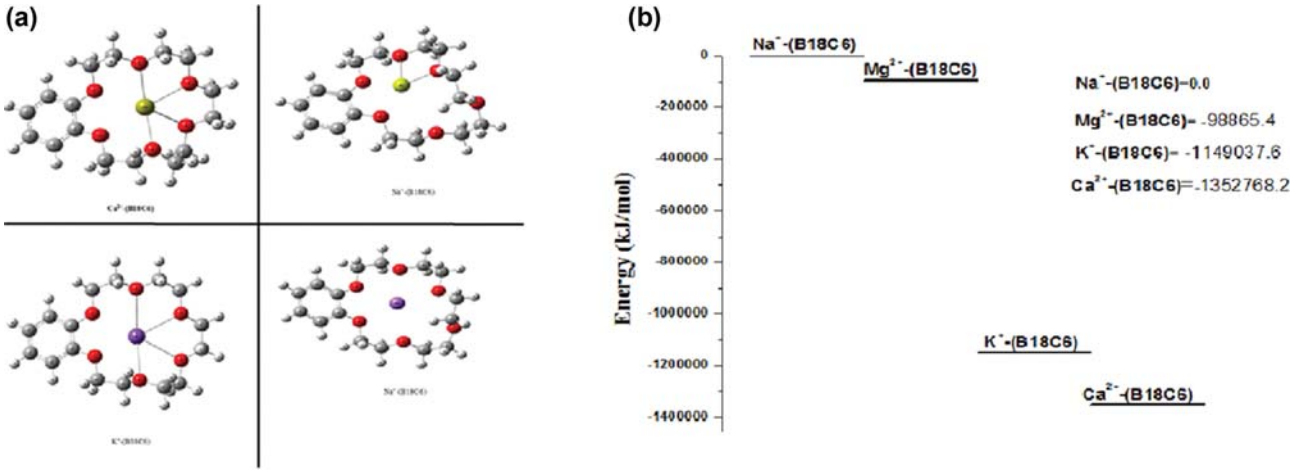

Fig. 17. (a) Optimized structures of different cations/crown ether complexes. (b) Free energies of different complexes of cations/crown ether at the B3LYP/6-311+g(d) level. All energy values are corrected by ZPE (zeropoint enery).

Table 3. Composition of different PIM in flux value

Polymer	Carrier	Plasticizer	Striping solution	Cation	J
CTA [8]	Dicyclohexano-18-crown-6	2-NPOE	Pure water	K	14
PVC [33]	Liquat 336 PIMs	-	HCl	Zn	24.8
PVDF [34]	-	Cyphos IL	NaOH	Cr	39.2
GPO (In this work)	B18C6	BMIMCl	Pure water	Ca	43.4

The hydrophobic character prevents the hydrated cations from entering the membrane, and as a consequence, the cations are allowed to transport via carrier molecules. Now, which cation does tend more to transport by carrier molecules? The experimental result was confirmed by calculation of the complex stability of cations/crown ether from density functional theory (DFT) employing the B3LYP/6-311+G (d) level of theory. Fig. 17 shows the thermodynamic parameters obtained in relation to the formation of different complexes of cations/crown ether.

As can be seen, the formation of the Ca^{+2}/crown ether complex is favored because the free energy of the product is more negative than that of Na^{+}, Mg^{+2}, K^{+} complexes with crown ether. Fig. 17(a) shows that two ions of Ca^{+2} and K^{+} each interact by coordination bonding with crown ether, while Mg^{+2} ion displays no bond with it, confirming the lowest transport flux of Na^{+} and Mg^{+} ions through the hydrophobic membrane.

6. Performance Comparison

So far, there is no report on calcium transport with PIM; therefore, the flux values for the transport of different cations with PIM prepared in this study and other PIMs in the literature are compared in Table 3.

As can be seen, the flux value in this study using GPO-based PIM was larger than that of other types of PIMs. However, we are not satisfied with this result, and for a better reason, the performance of GPO-based PIM in terms of the selectivity, stability and flux values was compared with PIM prepared by other competitive base polymer, i.e., PVC and PVDF under the same condition. For these three membranes of GPO-, PVC-, and PVDF-PIMs with the same composition as PIMC7 sample were prepared. Fig. 18 illustrates the selectivity values of these membranes regarding the calcium ion transport.

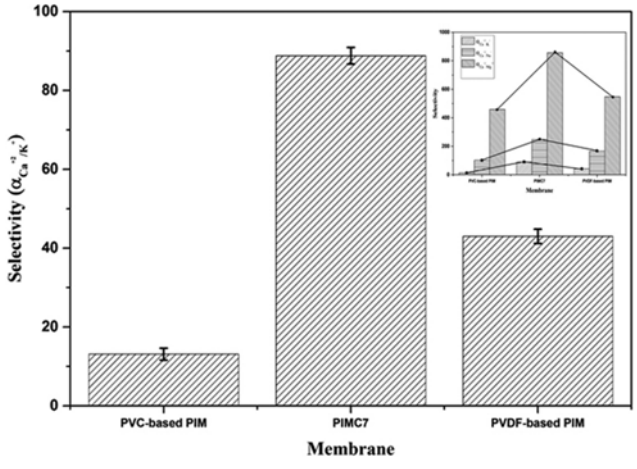

Fig. 18. Three membranes selectivities in bar graph, PIM7 and prepared membranes with similar compositions based on PVC and PVDF as competitors (Error bars are calculated but not clear here).

The unique properties of PIM7 due to the mentioned reasons cause a better selectivity compared with PVDF and PVC. To view better, the histogram of the selectivity of calcium ion over the potassium for three prepared membranes is superimposed in Fig. 18. The difference in selectivity can be seen here clearly. Comparing the contact angle measurements shows that the hydrophobicity of the surface of the GPO-based PIMs is nearly similar to that of PVDF-

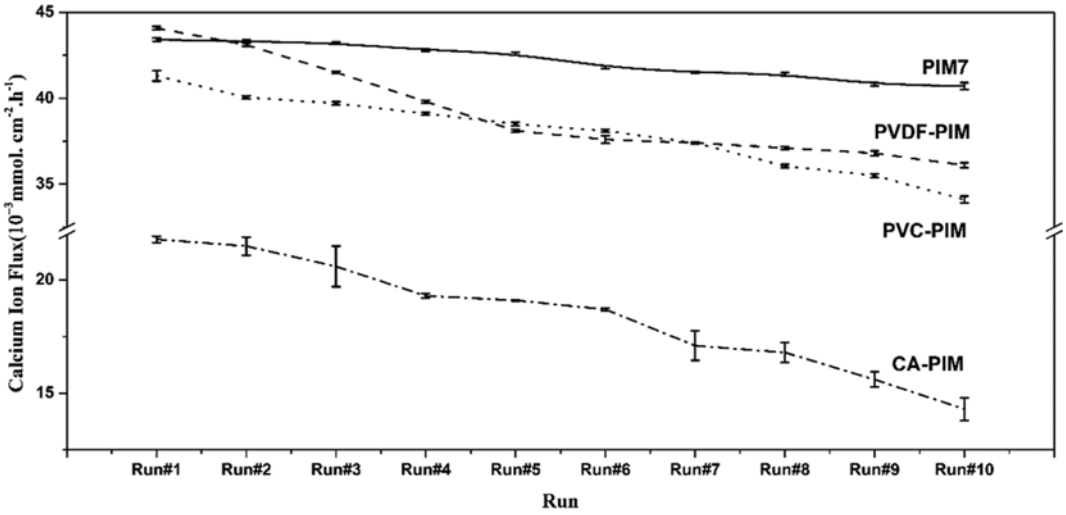

Fig. 19. Stability at various amounts of transfer fluxes for three membranes at different runs.

PIM (103±1°), while higher than that in PVC-PIM (89±1°).

The dynamic chemical stability of the membrane samples was characterized by the reusability of PIMs. The reusability of membranes was examined by repeating transport experiments so that both the aqueous feed and stripping phases were renewed over a certain period of time while the membrane was not changed. As can be seen from Fig. 19, the stability of GPO in comparison with the other two polymers is remarkably higher.

While the transport flux of calcium ion was decreased by only 5% after 10 runs for GPO-based PIM, the flux reduction reached 16, 15 and 34 percent of the initial flux value for PVDF-, PVC- and CA-PIMs, respectively. This means that reusing PVDF-, PVC- and CA-PIMs causes a high rate of flux reduction in membrane, but GPO-based membranes maintain well the selectivity and flux in more runs.

CONCLUSION

A novel reactive bio-polyols was synthesized from epoxidized castor oil and cellulose acetate as a polymer base for using in polymer inclusion membrane (PIM). The FTIR results strongly suggest that oxirane group in epoxidized castor oil molecules and the primary hydroxyl group of cellulose acetate has taken place. The study of XRD pattern peaks exhibits with reacting CA and epoxidized castor oil a fully amorphous structure is achieved, thereby indicating its potential application in PIM. The TGA data for the polymer degraded in nitrogen shows a higher initial and final decomposition temperature than the conventional cellulose acetate polymer base. We prepared a series of PIMs with different composition of green polyol, Ionic liquid (BMIMCl) and crown ether of B18C6. The influence of each component on the flux of Ca^{2+} and its competitive cations (K^+, Mg^{2+}, and Na^+) was investigated. The greatest flux and selectivity were observed when the ratio of crown ether versus PU was 0.75 and the content of ionic liquid (BMIMCl) was 1.5. Dynamic chemical stability experiments revealed the flux of Ca^{2+} transport was decreased from 43.4 to 39.2 (mmol·$cm^{-2}hr^{-1}$) after ten cycles; thus, flux was decreased only by 5% after ten cycles.

REFERENCES

1. M. L. Almeida, W. C. Robert and D. K. Spas, *Anal. Chim. Acta*, **1**, 987 (2017).
2. Y. Y. N. Bonggotgetsakul, R. W. Cattrall and S. D. Kolev, *Membranes*, **5**, 903 (2015).
3. N. A. Mamat and H. H. See, *J. Chromatogr. A*, **1406**, 34 (2015).
4. M. Regel-Rosocka, M. Rzelewska, M. Baczynska, M. Janus and M. Wisniewski, *Physicochem. Prob. Mi.*, **51** (2015).
5. M. Ershad, M. I. G. Almeida, T. G. Spassov, R. W. Cattrall and S. D. Kolev, *Sep. Purif. Technol.*, **195**, 446 (2018).
6. D. Wang, R. W. Cattrall, J. Li, M. Almeida, G. W. Stevens and S. D. Kolev, *J. Membr. Sci.*, **542**, 272 (2017).
7. B. Mahanty, P. Mohapatra, D. Raut, D. Das, P. Behere, M. Afzal and W. Verboom, *J. Environ. Chem. Eng.*, **4**, 1826 (2016).
8. A. Casadellà, O. Schaetzle and K. Loos, *Macromol. Rapid Commun.*, **37**, 858 (2016).
9. A. Shaaban, M. Azab, A. Mahmoud, A. Khalil and A. Metwally, *Desalin. Water Treat.*, **70**, 190 (2017).
10. B. M. Jayawardane, R. W. Cattrall and S. D. Kolev, *Anal. Chim. Acta*, **803**, 106 (2013).
11. C. A. Kozlowskia, J. Kozlowskia and W. Pellowski, *Desalination*, **321**, 119 (2013).
12. F. B. M. Suah, M. Ahmad and L. Y. Heng, *Spectrochim. Acta, Part A*, **144**, 81 (2015).
13. I. Pérez-Silva, C. A. Galán-Vidal, M. T. Ramírez-Silva, J. A. Rodríguez, G. A. Álvarez-Romero and M. E. Páez-Hernández, *Ind. Eng. Chem. Res.*, **52**, 4919 (2013).
14. G. Arena, A. Contino, A. Magri, D. Sciotto and J. Lamb, *Supramol. Chem.*, **10**, 5 (1998).
15. M. I. G. Almeida, C. Chan, V. J. Pettigrove, R. W. Cattrall and S. D. Kolev, *Environ. Pollut.*, **193**, 233 (2014).
16. K. Witt, E. Radzyminska-Lenarcik, A. Kosciuszko, M. Gierszewska and K. Ziuziakowski, *Polymers*, **10**, 134 (2018).
17. M. I. G. Almeida, R. W. Cattrall and S. D. Kolev, *J. Membr. Sci.*, **415**, 9 (2012).
18. E. A. Nagul, C. Fontàs, I. D. McKelvie, R. W. Cattrall and S. D. Kolev,

Anal. Chim. Acta, **803**, 82 (2013).
19. T. Ohshima, S. Kagaya, M. Gemmei-Ide, R. W. Cattrall and S. D. Kolev, *Talanta*, **129**, 564 (2014).
20. B. Pospiech, *Sep. Sci. Technol.*, **49**, 1706 (2014).
21. S. Chaudhury, A. Bhattacharyya and A. Goswami, *Environ. Sci. Technol.*, **48**, 12994 (2014).
22. F. B. M. Suah, M. Ahmad and L. Y. Heng, S*ens. Actuators, B*, **201**, 490 (2014).
23. B. Pospiech, *J. Solution Chem.*, **44**, 2431 (2015).
24. F. Tomás-Alonso, A. M. Rubio, R. Álvarez and J. A. Ortuño, *Int. J. Electrochem. Sci.*, **8**, 4955 (2013).
25. B. Pospiech, *Physicochem. Probl. Mi.*, **51**, 281 (2015).
26. A. Kaya, C. Onac, H. K. Alpoguz, A. Yilmaz and N. Atar, *Chem. Eng. J.*, **283**, 141 (2016).
27. C. J. Malm, L. Tanghe, B. C. Laird and G. D. Smith, *Anal. Chem.*, **26**, 188 (1954).
28. Y. O'Bryan, R. W. Cattrall, Y. B. Truong, I. L. Kyratzis and S. D. Kolev, *J. Membr. Sci.*, **510**, 488 (2016).
29. M. I. G. Almeida, A. M. Silva, R. A. Coleman, V. J. Pettigrove, R. W. Cattrall and S. D. Kolev, *Anal. Bioanal. Chem.*, **408**, 3213 (2016).
30. Y. Y. N. Bonggotgetsakul, R. W. Cattrall and S. D. Kolev, *J. Membr. Sci.*, **514**, 274 (2016).
31. I. Zawierucha, C. Kozlowski and G. Malina, *Waste Manage.*, **33**, 2129 (2013).
32. B. Pospiech, *Physicochem. Probl. Mi.*, **49**, 641 (2013).
33. C. V. Gherasim and G. Bourceanu, *Chem. Eng. J.*, **220**, 24 (2013).
34. I. Zawierucha, C. Kozlowski and G. Malina, *Waste Manage.*, **33**, 2129 (2013).
35. N. S. Abdul-Halim, P. G. Whitten and L. D. Nghiem, *Sep. Purif. Technol.*, **119**, 14 (2013).
36. L. Guo, Y. Liu, C. Zhang and J. Chen, *J. Membr. Sci.*, **372**, 314 (2011).